Journal of Fluorescence, Vol. 2, No. 2, 1992

Direct and Reverse Energy Transport in Systems of Monomers and Imperfect Traps: Monte Carlo Simulations

Leszek Kułak[1] and Czesław Bojarski[1]

Received May 8, 1992; accepted August 18, 1992

A Monte Carlo simulation of the concentration dependence of the fluorescence quantum yield η_M and emission anisotropy r_M of a system containing dye molecules in the form of monomers M and clusters T (statistical pairs and trimers) playing the role of the imperfect traps for nonradiative excitation energy transfer (NET) has been carried out. The simulation has been made for determined values of Förster critical distances R_0^{MM} and R_0^{MT} and for several values of R_0^{TM} and R_0^{TT}, assuming that the energy may be transferred from M* to T as well as from T* to M (reverse nonradiative energy transfer, RNET). It was shown that the RNET process in the range of high concentrations may strongly change the values of r_M as well as those of η_M. For emission anisotropy r_M an effect of repolarization was observed which decreases rapidly with increasing R_0^{TM} and R_0^{TT}. A very good agreement between the simulation results of η_M and the theoretical model with no adjustable parameters was found. In the model, the RNET process and influence of correlation between active molecules on energy migration among monomers were taken into account.

KEY WORDS: Energy transfer; quantum yield; emission anisotropy; Monte Carlo simulation.

INTRODUCTION

The process of fluorescence concentration quenching (FCQ) in solution is often related to nonradiative electronic excitation energy transport (NET) from monomers M (donors) to ground-state dimers or statistical pairs of luminescent molecules treated as perfect traps T (acceptors) for the excitation energy [1–4]. Recently [5] the FCQ process in solution was investigated under the assumption of energy transport in one direction from excited monomers to statistical pairs—perfect traps with the quantum yield $\eta_{0T} = 0$. It was shown [6] that the absorption spectrum of monomers M significantly overlaps the fluorescence (FL) spectrum of traps T and that a measurable FL quantum yield η_{0T} is observed even in the solutions of low viscosity (imperfect traps). This fact allows reverse nonradiative energy transfer (RNET) from excited traps T* to monomers M. Recent studies [7] of the rise in FL decay time with the increase in solution viscosity may suggest that the quantum yield of the traps should also increase. Hence, the transport of excitation energy in a system of molecules M and T is possible in both directions, M*→T and T*→ M [8]. Suitable conditions for the RNET process are found, for example, in photosystems of green plants, where the excited trap can depopulate via excitation detrapping to chlorophyll [9]. It has been shown there that the detrapping process is important and should not be neglected. A similar RNET process can be significant in the case of other donor and acceptor molecular systems, with closely located first excited singlet levels. Examples are chlorophyll forms [10], fractions of luminescent molecules in inhomogeneously broadened systems [11], and monomer- and ground-state dimer systems with $\eta_{0T} > 0$ (luminescent dimers [12,13]). Large overlapping of monomer and dimer spectra is inherently connected with exciton splitting

[1] Department of Technical Physics and Applied Mathematics, Technical University of Gdańsk, Majakowskiego 11/12, 80-952 Gdańsk, Poland.

1053-0509/92/0600-0123$06.50/0

of the first excited M* energy level [14]. Taking this into account, one may expect reverse energy transfer to take place in systems of high donor concentrations [8]. As recently shown, the RNET process may significantly affect the monomer fluorescence quantum yield η_M when the overlap integral J_{TM} and trap fluorescence yield η_{0T} are large enough [15,16]. A similar influence on emission anisotropy, fluorescence decay, and FL average decay time can be expected [17,18].

Large overlapping of absorption and fluorescence bands of donor and acceptor leading to reabsorption and secondary fluorescence makes experimental verification of the RNET effect upon luminescence characteristics of molecular systems difficult. These secondary effects can be eliminated by using sufficiently thin layers of the luminophore [19] or by taking into account, on the basis of a suitable theory, the influence of these effects on the luminescent properties of solutions [20,21]. Determining the concentration of traps in a system with a weak concentration dependence of absorption spectra may be an additional difficulty in experimental investigations. Therefore investigation of the RNET process has been undertaken by means of a Monte Carlo simulation.

In this paper we present a method of simulation of the steady-state quantum yield and emission anisotropy of a system containing monomers and imperfect traps. The numerical results and their comparison with the heuristic hopping model are presented. We also compare our model with that of Knoester and Van Himbergen [5] in the case of perfect traps and discuss the model with imperfect traps.

METHOD OF SIMULATION

In simulation, N luminescent molecules (LM) of dimensionless reduced density $\hat{\gamma}$ ($\hat{\gamma} = C/C_0^{MM}$, where C is the analytical concentration and C_0^{MM} is the monomer critical concentration) were randomly distributed in a three-dimensional cube. The excitation energy can be transferred to any other LM and the transfer rates are taken to be independent of orientation and only dependent on distance. Any two molecules within distance R_T of one another are assumed to form an imperfect trap (statistical pair with $\eta_{0T} > 0$). Moreover, for high densities, higher-order clusters appear, but only statistical trimers are taken into account (the configurations at which other clusters appear are rejected). The monomer molecules are labeled 1 through N_m, molecules in statistical pairs $N_m + 1$ through $N_m + 2N_p$ and in statistical trimers $N_m + 2N_p + 1$ through N, where the numbers of pairs and trimers are N_p and N_t, respectively. The probability that an excitation is on the jth molecule in fixed configuration at time t, $p_j(t)$, satisfies the master equation [22]

$$\frac{d\mathbf{P}}{dt} = -\mathbf{W} \circ \mathbf{P} \tag{1}$$

where $\mathbf{P}$ is a vector with components $[p_1(t), p_2(t), \ldots, p_{N_c}(t)]$ and $\mathbf{W}$ is an $N_c \times N_c$ matrix ($N_c = N_m + N_p + N_t$) given by

$$W_{jk} = -w_{jk}^{MM} + \delta_{jk}\left[\sum_{l=1}^{N_m} w_{lk}^{MM} + \sum_{l=N_m+1}^{N_c} w_{lk}^{MT}\right], \qquad j \le N_m, \quad k \le N_m$$

$$W_{jk} = -w_{jk}^{MT}, \qquad N_m + 1 \le j \le N_c, \quad k \le N_m$$

$$W_{jk} = -w_{jk}^{TM}, \qquad j \le N_m, \quad N_m + 1 \le k \le N_c$$

$$W_{jk} = -w_{jk}^{TT} + \delta_{jk}\left[\sum_{l=1}^{N_m} w_{lk}^{TM} + \sum_{l=N_m+1}^{N_c} w_{lk}^{TT}\right], \qquad N_m + 1 \le j \le N_c, \quad N_m + 1 \le k \le N_c$$

The distance-dependent transfer rates between two monomer molecules and a monomer and a trap molecule (the statistical pair and the trimer) are given by w_{jk}^{MM}, w_{jk}^{MT} ($w_{jj}^{XX}, X \in \{M,T\}$ are assumed to be zero). The back-transfer rate between a trap and a monomer molecule is defined as w_{jk}^{TM} and the transfer rate between two traps is w_{jk}^{TT}. The transfer rates w_{jk}^{XX}, $X \in \{M,T\}$, are assumed to be symmetric and defined as the orientation averaged Förster rate, applicable to a dipole–dipole interaction [23],

$$w_{jk}^{MX} = \frac{1}{\tau_{0M}}\left(\frac{R_0^{MX}}{r_{jk}}\right)^6, \quad w_{jk}^{TY} = \frac{1}{\tau_{0T}}\left(\frac{R_0^{TY}}{r_{jk}}\right)^6, \quad X, Y \in \{MT\} \tag{2}$$

R_0^{MM}, R_0^{MT}, R_0^{TM} and R_0^{TT} are the respective Förster distances for monomer–monomer, monomer–trap, trap–monomer, and trap–trap excitation transfers; τ_{0M} and τ_{0T} are the intrinsic monomer and trap excitation lifetimes. The quantities of interest here are the relative emission r_M/r_{0M} anisotropy and the relative quantum yield η_M/η_{0M}, given by [5]

$$r_M/r_{0M} = \left\langle \sum_i^{Nm} [(\mathbf{I} + \tau_{0M}\mathbf{W})^{-1}]_{ii} / \sum_{i,j}^{Nm} [(\mathbf{I} + \tau_{0M}\mathbf{W})^{-1}]_{ij} \right\rangle \tag{3}$$

$$\eta_M/\eta_{0M} = \left\langle \sum_{i,j}^{Nm} [(\mathbf{I} + \tau_{0M}\mathbf{W})^{-1}]_{ij} \right\rangle / N_m \tag{4}$$

where the symbol $\langle \cdots \rangle$ denotes the average over all possible configurations of donors and traps, and $\mathbf{I}$ is an identity matrix. The inverse matrix of $\mathbf{I} + \tau_{0M}\mathbf{W}$ cannot be calculated analytically but can be exploited very well in the Monte Carlo simulation.

The dependence of quantities of interest on density $\hat{\gamma}$ for a given monomer configuration is obtained by rescaling critical radii for energy transfer, keeping the length of the box edge equal to 1. The pseudo-random number generator, which passed several statistical tests, was also verified by checking the simulated trap density against the analytically expected value. Traps are detected by calculating all intermolecular distances and comparing them to the statistical pair radius. The effects of the finite size of the generated configurations are reduced by introducing periodic boundary conditions (the box is surrounded by replicas of itself) with a minimum image convention (the donor or the trap interacts with another molecule, the latter being an original molecule or a periodic image). Next the number N_m of monomers is obtained and the $N_c \times N_c$ matrix $\mathbf{I} + \tau_{0M}\mathbf{W}$ is filled. This matrix is not symmetrical and is defined as positive. Its inverse matrix is calculated using standard numerical procedures. Then, after a suitable number of simulated runs, averaged quantities of interest are calculated. The number of molecules N for individual simulation runs is limited by CPU time consumption and numerical stability. After performing several convergence tests, N = 300 was chosen as a sufficient number of molecules. Numerical results for the relative quantum yield and emission anisotropy were generated for densities varying from $\hat{\gamma} = 0.03$ to $\hat{\gamma} = 100$. The number of necessary simulated configurations depends on the density. Therefore, at low densities ($\hat{\gamma} < 1$), 2000 runs of 300 molecules were sampled, while for intermediate densities ($1 < \hat{\gamma} < 50$), 3000 runs of 300 molecules were made. At very high densities ($\hat{\gamma} > 50$), because of the strong dependence of emission anisotropy on the number of molecules, 2000 runs of 500 molecules were performed. The nonsymmetrical matrices $\mathbf{I} + \tau_{0M}\mathbf{W}$ were inverted by the Gauss procedure, which was tested to show whether a system with no traps gives a quantum yield equal unity. For N up to 600, the observed deviations were very small for all densities (maximal error, less than 0.01%).

NUMERICAL RESULTS

Quantum Yield

The numerical results for relative quantum yield, for the system containing monomers and statistical traps whose imperfection is characterized by parameter R_0^{TM}, are shown in Fig. 1. The numerical results were obtained for the values of parameters listed in Table I. The values of R_0^{MT}, R_0^{TM}, and R_0^{TT} were obtained from the fluorescence and absorption spectra of monomers and traps taken

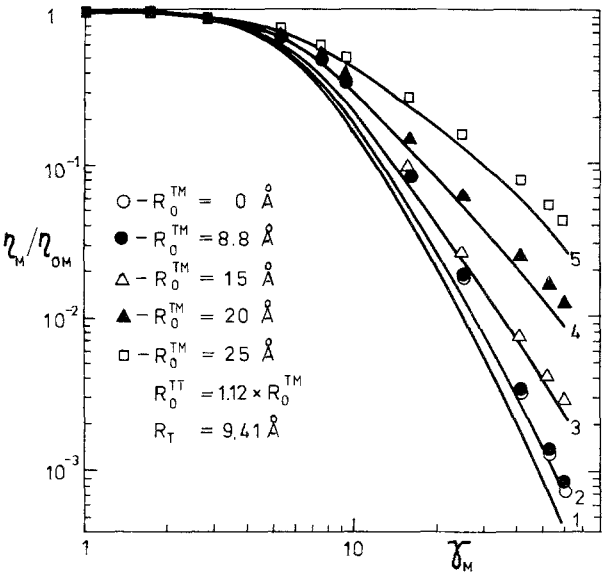

Fig. 1. Quantum yield η_M/η_{0M} versus reduced monomer concentration $\gamma_M = (\sqrt{\pi}/2)(C_M/C_0^{MM})$; ○, ●, △, ▲, and □ are results of Monte Carlo simulations for parameters listed in Table I and different values of R_0^{TM} and R_0^{TT}. Curves 1–5, corresponding to the increasing values of R_0^{TM} and R_0^{TT}, were computed from Eq. (5) with denotations (6)–(9), (12), and (13) for the same parameters. The model is without correlations.

from Ref. 6. Critical radius R_0^{MM} was taken from Ref. 24 and the distance between dye molecules in a pair R_T was accepted as in Ref. 3. All critical radii were determined for rhodamine 6G in methanol with an orientation factor $\kappa^2 = 2/3$ [25]. The values of R_0^{MM} and R_0^{MT} are close to those obtained for rhodamine 6G in viscous and solid solutions [26,27] (difference does not exceed 10%). Thus, the values of parameters assumed in the Monte Carlo simulation are attainable for realistic physical systems. Let us note that very small values of R_0^{TM} and R_0^{TT} are brought out by a small value of η_{0T} in methanol (see Table I). In solutions of elevated viscosity an increase in η_{0T} as well as in R_0^{TM} and R_0^{TT} should be expected. The simulation results for the values of parameters presented in Table I are shown as filled circles in Fig. 1 (R_0^{TM} = 8.8 Å). The values of η_M/η_{0M} differ from corresponding values for the system with perfect traps (R_0^{TM} = 0 Å) only for the highest concentrations. All other simulation results for relative quantum yield are obtained for parameters listed in Table I as previously but for several values of R_0^{TM} and R_0^{TT}. The results considerably exceed the values of η_M/η_{0M} obtained for R_0^{TM} = 0 Å and show that in the range of high concentrations ($\gamma_M > 10$), the influence of the RNET process on the quantum yield may be significant. The results obtained

Table I. The Values of Energy Transfer Parameters for the System Investigated.

R_0^{MM} (Å)	R_0^{MT} (Å)	C_0^{MM} ($\times 10^{-3}$ mol/dm^3)	C_0^{MT} ($\times 10^{-3}$ mol/dm^3)	η_{0M}[a]	R_0^{TT} (Å)	R_0^{TM} (Å)	C_0^{TT} ($\times 10^{-3}$ mol/dm^3)	C_0^{TM} ($\times 10^{-3}$ mol/dm^3)	η_{0T}	R_T (Å)
55.4	51.8	2.33	2.87	0.85	9.87	8.8	4.13	5.82	0.0085	9.41

[a]Taken from Ref. 28.

have been compared with theoretical expression, taking into account the forward and reverse energy transfer between monomers and traps as well as energy migration in the form [8,17,18]

$$\eta_M/\eta_{0M} = \frac{1 - f(\gamma)}{1 - \alpha f(\gamma)} \frac{1}{1 - B} \tag{5}$$

$$B = \frac{(1 - \alpha)f(\gamma)}{1 - \alpha f(\gamma)} \frac{(1 - \bar{\alpha})f(\bar{\gamma})}{1 - \bar{\alpha} f(\bar{\gamma})} \tag{6}$$

$$f(\gamma) = \pi^{1/2}\gamma \exp(\gamma^2)[1 - \mathrm{erf}(\gamma)] \tag{7}$$

$$\begin{aligned} \gamma &= \gamma_M + \gamma_T \\ &= (\pi^{1/2}/2)(C_M/C_0^{MM} + C_T/C_0^{MT}); \\ \alpha &= \gamma_M/\gamma \end{aligned} \tag{8}$$

$$\begin{aligned} \bar{\gamma} &= \bar{\gamma}_M + \bar{\gamma}_T \\ &= (\pi^{1/2}/2)(C_M/C_0^{TM} + C_T/C_0^{TT}); \\ \bar{\alpha} &= \bar{\gamma}_T/\bar{\gamma} \end{aligned} \tag{9}$$

where C_M and C_T are the concentrations of M and T molecules. $C_0^{XY} = (3/4\pi)/(R_0^{XY})^3$, $X,Y \in \{M,T\}$, denotes the critical concentration for the NET process from X^* to Y and can be obtained from the relation [23]

$$C_0^{XY} = 4.23 \cdot 10^{-10} n^2 (\eta_{0X} \bar{\kappa}^2 J_{XY})^{-1/2} \quad (\mathrm{mol/dm^3}) \tag{10}$$

where

$$J_{XY} = \int_0^\infty f_x(\nu)\epsilon_Y(\nu)\frac{d\nu}{\nu^4} \tag{11}$$

is the overlap of the X molecule fluorescence spectral distribution $f_x(\nu)$ expressed as the number of quanta and normalized to unity, $\epsilon_Y(\nu)$ is the Y molecule extinction coefficient, n is the refractive index of the medium, ν is the wave number, and κ^2 is the orientation factor.

As can be seen from Eqs. (8) and (9), $\bar{\gamma}$ and $\bar{\alpha}$ can be expressed by γ and α:

$$\begin{aligned} \bar{\gamma} &= \gamma[1 - \alpha(1 - b)]C_0^{MT}/C_0^{TT} \\ \bar{\alpha} &= (1 - \alpha)/[1 - \alpha(1 - b)] \end{aligned} \tag{12}$$

where

$$b = C_0^{TT}C_0^{MM}/(C_0^{TM}C_0^{MT}) \tag{13}$$

Thus, taking critical concentrations C_0^{XY} as given constants, the relative quantum yield η_M/η_{0M} proves to be a function of the reduced concentration γ and the ratio α (or γ_M and γ_T). When quantum yield $\eta_{0T} = 0$ or overlap integral $J_{TM} = 0$, a reverse transfer of energy does not occur. In such a case, $B = 0$ [Eqs. (10) and (6) to (9)] and Eq. (5) becomes [29,30]

$$\eta_M/\eta_{0M} = \frac{1 - f(\gamma)}{1 - \alpha f(\gamma)} \tag{14}$$

In Fig. 1 the numerical values η_M/η_{0M} are compared with the theoretical curves calculated from Eq. (5). Curves 2–5 correspond to the case when the RNET process is taken into consideration, and curve 1 to the case when it is neglected. Only the values of η_M for $R_T = 8.8$ Å lie relatively close to curve 1. For larger R_T, numerical points are significantly shifted away from curve 1. These points also differ distinctly from corresponding theoretical curves. This suggests that the effectiveness of excitation energy trapping calculated from Eq. (5) is too high. This is likely to occur since Eq. (5) was obtained assuming that no statistical correlation exists between configurations surrounding the excited monomer molecule before and after the hopping act. However, the partial consideration of these correlations in the process of monomer–monomer energy transfer by means of the method introduced by Huber *et al.* [31,32] and applied in the NET theory in Refs. 33 and 34 leads to the replacement of concentration γ_M in Eq. (5) by a smaller concentration $\gamma_M/\sqrt{2}$ (hopping model with correlations). In Fig. 2, numerical results from Fig. 1 are compared with Eq. (5) after replacing γ and α from Eq. (8) and $\bar{\gamma}$ and $\bar{\alpha}$ from Eq. (9) by

$$\gamma' = \gamma_M/\sqrt{2} + \gamma_T; \qquad \alpha' = \gamma_M/(\sqrt{2}\gamma') \tag{8'}$$

$$\bar{\gamma}' = \bar{\gamma}_M + \bar{\gamma}_T/\sqrt{2}; \qquad \bar{\alpha}' = \bar{\gamma}_T/(\sqrt{2}\bar{\gamma}') \tag{9'}$$

respectively. Now curves 3′–5′, corresponding to the same values of parameters as curves 3–5 in Fig. 1, are in a very good agreement with numerical results for all

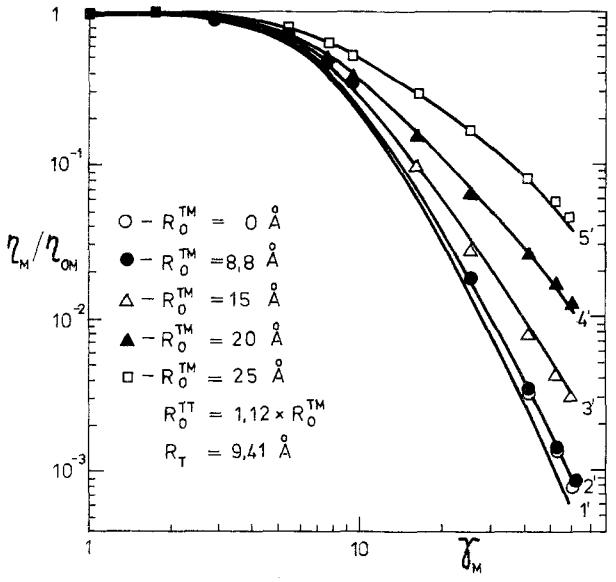

Fig. 2. Numerical results as in Fig. 1. Curves 1'–5' were computed from Eq. (5) with denotations (8) and (9) substituted by (8') and (9'). The model is with correlations.

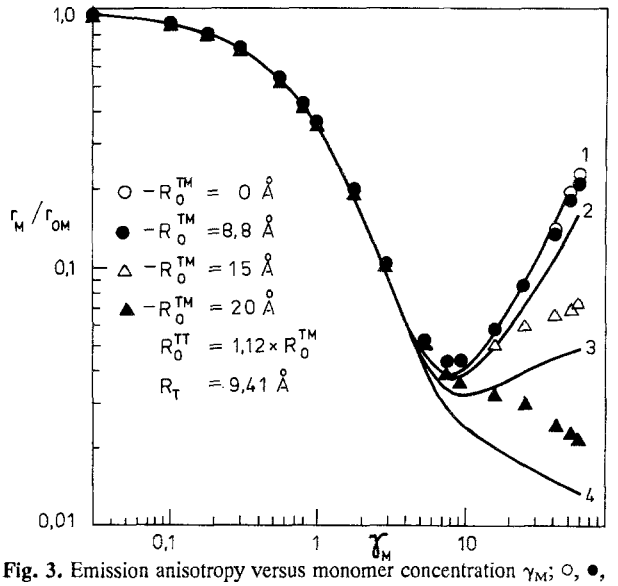

Fig. 3. Emission anisotropy versus monomer concentration γ_M; ○, ●, △, and ▲ are results of Monte Carlo simulations for parameters from Table I and different values of R_0^{TM} and R_0^{TT}. Curves 1–4 were calculated for the same values of parameters from Eq. (17).

concentrations, whereas curves 1 and 2 show a reduced coincidence with them. This is especially evident for the system with no back-transfer (R_0^{TM} = 0 Å).

Emission Anisotropy

We have also carried out Monte Carlo simulation of the concentration dependence of emission anisotropy r_M for the system discussed in the previous paragraph. Numerical results for r_M obtained for values of parameters from Table I and for different values of R_0^{TM} and R_0^{TT} are presented in Fig. 3. For perfect traps (R_0^{TM} = 0 Å) as well as for "almost"-perfect traps (R_0^{TM} = 8.8 Å), the emission anisotropy rises in the region of highest concentrations, which is due to strong concentration quenching (cf. results of η_M/η_{0M} simulation in Fig. 1). One can notice that the effect of reverse energy transfer for $R_0^{TM} > 15$ Å is significant in this concentration region and the repolarization effect practically disappears. For increasing R_0^{TM} values, a significant portion of excitations reaching the traps returns to the set of monomer molecules and is subsequently emitted as nonpolarized fluorescence. Similarly as in the case of quantum yield, it would be interesting to compare numerical results for the emission anisotropy with a suitable theoretical expression. Unfortunately, such an expression is not known and its accurate derivation seems difficult. In the case of random and uniform spatial distribution of the molecular dipole directions in space, it has commonly been assumed in theories of concentration depolarization of fluorescence (CDF) that only molecules M_i, excited primarily by light absorption, contribute to the observed emission anisotropy [35,36]. In this case [29,37]

$$r_M/r_{0M} = \eta_i/\eta_M \tag{15}$$

where η_i is the fluorescence quantum yield of molecules M_i, and η_M is the total fluorescence yield.

The fact that excitation energy, originally localized on the M_i molecule, may migrate as a localized exciton between M_i molecules from the surroundings of the M_i molecule and may repeatedly return to it should be taken into account when calculating η_i. Thus, to the quantum yield, η_i contribute not only M_i molecules excited by absorption of light (m = 0) but also M_i molecules excited after m steps of nonradiative transfers (m = 2,3,...).

Taking into account the returns of excitation to M_i, we have obtained [33]

$$\eta_i/\eta_{0M} = 1 - f(\gamma') \tag{16}$$

where γ' is defined in (8') and $f(\gamma')$ in (7).

This expression takes into account the correlations mentioned above as well as the energy transfer to traps but without the possibility of its returning to monomers. However, an approximate result for emission anisotropy may be obtained under the simplifying assumption that the excitation energy transferred from traps to monomer

molecules affects only the total fluorescence yield η_M and does not influence the fluorescence quantum yield η_i of monomers M_i initially excited by light absorption. For the total fluorescence yield η_i we accept Eq. (5) with denotations (6)–(9), where expressions (8) and (9) are replaced by (8′) and (9′), namely,

$$\eta_M/\eta_{0M} = \frac{1 - f(\gamma')}{1 - \alpha' f(\gamma')} \frac{1}{1 - B'} \tag{5'}$$

where

$$B' = \frac{(1 - \alpha')f(\gamma')}{1 - \alpha' f(\gamma')} \frac{(1 - \bar{\alpha}')f(\bar{\gamma}')}{1 - \bar{\alpha}' f(\bar{\gamma}')} \tag{6'}$$

Taking into account expressions (15), (16), and (5′), we obtain

$$r_M/r_{0M} = \eta_i/\eta_M = [1 - \alpha' f(\gamma')](1 - B') \tag{17}$$

Curves 1–4 calculated according to Eq. (17) for values of parameters from Table I are shown in Fig. 3. Curve 1 corresponds to the system in which reverse energy transfer does not occur [$R_0^{TM} = 0$ Å and $B' = 0$ in Eq. (17)]. Numerical values of r_M/r_{0M} obtained for $R_0^{TM} > 0$ deviate distinctly from curve 1 in the highest concentration range, thus evidencing the reverse transfer. However, they lie slightly above the calculated curves, as one could expect on account of the simplifications made. This proves that some of the excitations transferred from traps reach molecules M_i.

DISCUSSION

A simple model of concentration self-quenching of luminescence due to incoherent energy transfer to the statistical pairs treated as perfect traps has been discussed by Knoester and Van Himbergen [5]. They carried out the numerical calculations of the yield η_M and emission anisotropy r_M by applying the Monte Carlo simulation in a three-dimensional space for $R_T/R_0^{MM} = 0.2$, $\eta_{0M} = 1/3$, and reduced concentrations from $\hat{\gamma} = 0.05$ up to $\hat{\gamma} = 100$. In the present work a very similar method of Monte Carlo simulation is adopted. Thus, it is of interest to compare our numerical results for η_M and r_M, with $R_0^{TM} = 0$ Å, with the mentioned data. The numerical results were obtained by us for the same values $R_T = 10$ Å and $R_0^{MM} = 50$ Å as in Ref. 5. As mentioned before, monomers, statistical pairs, and trimers are considered in present work. Other clusters were rejected, opposite to the model presented in Ref. 5, which describes all clusters. We have stated that the results of both simulations coincide for nearly the whole range of densities. Only for the highest densities do the emission anisotropy values just exceed those from Ref. 5. Hence, clusters composed of four or more monomers practically do not affect the numerical results. Curve 1 in Fig. 4A has been obtained in the same way as in Ref. 5 from formula (14) for $C_0^{MM} = (3/4\pi)/(R_0^{MM})^3 = 0.00317$ mol/dm^3 ($R_0^{MM} = 50$ Å) and for $C_0^{MT} = C_0^{MM}/\sqrt{2}$. The value of the critical concentration C_0^{MT} mentioned above arises from the assumption that the transfer rate for the transfer process from M* to T is given by

$$w_{ij}^{MT} = 2w_{ij}^{MM} = (2/\tau_{0M})(R_0^{MM}/r_{ij})^6 \tag{18}$$

Concentrations C_M and C_T have been determined from the expressions

$$C_M = x_M C \quad \text{and} \quad C_T = x_T C/2 = (1 - x_M)C/2 \tag{19}$$

with

$$x_M = \exp(-\mu) \quad \text{and} \quad \mu = V_T N_A C \tag{20}$$

where μ is the average number of monomers in a volume $V_T = (4/3)\pi R_T^3$, and N_A is Avogadro's number. It follows from Eq. (18) that in Ref. 5, monomers clustered in groups of two or more molecules have been treated as statistical pairs with the same transfer rate. As shown in Fig. 4A, values of η_M/η_{0M} represented by curve 1 are evidently too low.

For more precise analysis, higher-order clusters M_n besides monomers $M = M_1$ and pairs $T = M_2$ have been taken into account. The cluster M_n is composed of n monomers and is characterized by concentration C_n and critical concentration C_{0n} for the NET process from M* to M_n with rate a constant w_n. These concentrations have been obtained from the following equations:

$$C_n = (C/n)(\mu^{n-1}/(n-1)!)\exp(-\mu) \tag{21}$$

and

$$C_{0n} = C_0^{MM}/\sqrt{n}, \qquad n = 1,2,3... \tag{22}$$

where the transfer rate for the NET process was taken as $w_n = nw_{ij}^{MM}$. Curve 2 was calculated from Eq. (14) under the assumption that monomers, pairs, and also trimers were present in the system. In this case, quantities γ and α are determined from relation (23) for $p = 3$:

$$\gamma = \sum_{n=1}^{p} \gamma_n = (\sqrt{\pi}/2)\hat{\gamma} \exp(-\mu) \sum_{n=1}^{p} \mu^{n-1}/((n-1)!\sqrt{n})$$

with

$$\alpha = \gamma_1/\gamma \quad \text{and} \quad \hat{\gamma} = C/C_0^{MM} \tag{23}$$

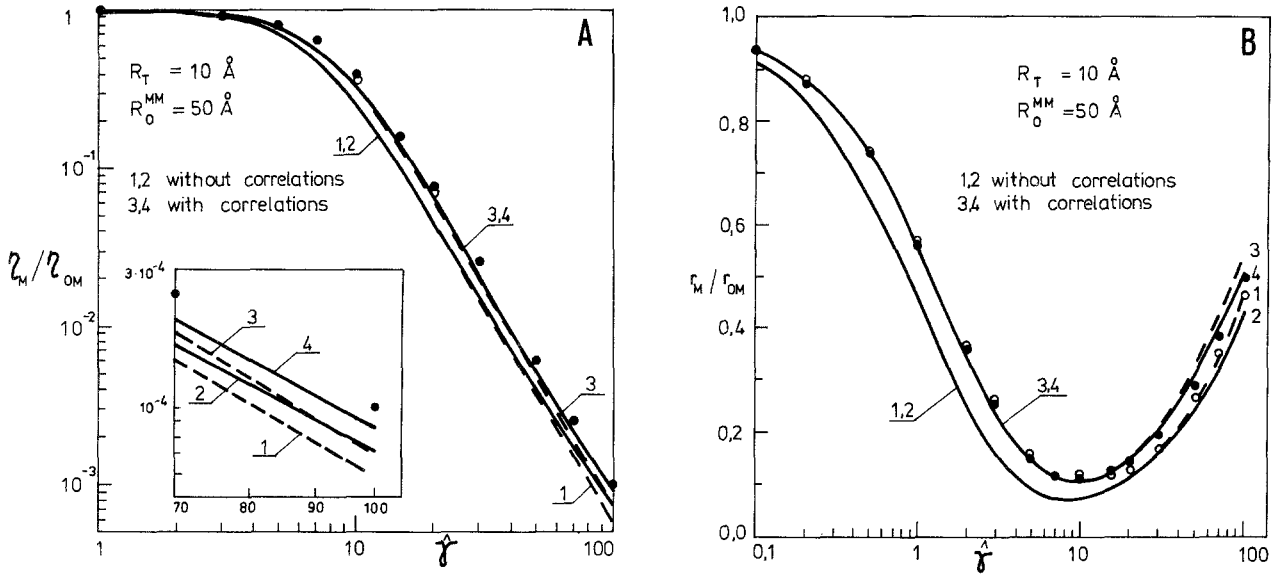

Fig. 4. (A) Quantum yield η_M and (B) emission anisotropy r_M versus concentration $\hat{\gamma} = C/C_0^{MM}$; • and ○ are Monte Carlo simulations performed in this work and in Ref. 5, respectively. (A) Curves 1, 2, 3, and 4 were computed from Eq. (14); (B) curves 1, 2, 3, and 4 were computed from Eq. (26). Curves 1, 2, 3, and 4: γ and α from Eqs. (8), (23), (24), and (25), respectively. Curves 1 and 3—traps: all clusters M_n ($n > 2$) treated as statistical pairs. Curves 2 and 4—traps: statistical pairs and trimers.

This time the numerical data also differ from curve 2. However, the hopping model with correlations considerably improves the agreement between theoretical and numerical results. Curves 3 and 4 in Fig. 4A were calculated from Eq. (14) after replacing γ and α from Eq. (8) with

$$\gamma = \gamma_M/\sqrt{2} + \gamma_T \quad \text{and} \quad \alpha = \gamma_M/(\sqrt{2}\gamma) \quad (24)$$

and

$$\gamma = \gamma_1/\sqrt{2} + \gamma_2 + \gamma_3 \quad \text{and} \quad \alpha = \gamma_1/(\sqrt{2}\gamma). \quad (25)$$

respectively. Curve 4 has been calculated assuming that the system contains trimers, in addition to monomers and statistical pairs. The simulation results of the emission anisotropy r_M for the systems discussed above are presented in Fig. 4B. The results have been compared with theoretical curves calculated from Eq. (26) [29],

$$r_M/r_{0M} = 1 - \alpha f(\gamma) \quad (26)$$

which does not take into account the statistical correlations similarly as Eq. (14) for quantum yield.

The quantities α and γ for curves 1, 2, 3, and 4 were determined from Eqs. (8), (23), (24), and (25), respectively. Curves 3 and 4 correspond to the hopping model in which correlations were considered, and curves 1 and 2 when they were neglected. One can see that the simulation results for r_M evidently differ from curves 1 and 2 and lie very well along curve 4 for all densities. They also fit curve 3 well except for the last three points.

From the above discussion it follows that taking into account statistical pairs and trimers as perfect traps and appropriate characterization of their quenching strength by different critical radii, the concentration dependence of η_M and r_M is better described than in the case when the model treating all clusters as statistical pairs with the same quenching strength is applied. Needless to say, in the range of $\hat{\gamma} < 10$ discrepancies are small (see curves 3 and 4 in Fig. 4A) and appear only for higher densities.

Let us note that expressions (14) and (26) have been successfully applied to describe the concentration quenching in monomer/ground-state dimer systems [26,38–41]. They have identical form and content as Eqs. (37a) and (37b) obtained later in Ref. 4.

We have shown [42,43] that the hopping model with correlations gives for η_M and r_M results surprisingly close to those obtained in the framework of the systematic LAF (Loring, Andersen, Fayer) theory [22].

On the other hand, the very good agreement of the Monte Carlo data for η_M with the theoretical results (Fig. 2) shows that the model with correlations may also be successfully applied to the quantitative description of a system with imperfect traps. Therefore it is worthwhile discussing the influence of the trap radius R_T and critical radii R_0^{TM} and R_0^{TT} on the yield η_M. Figure 5 presents

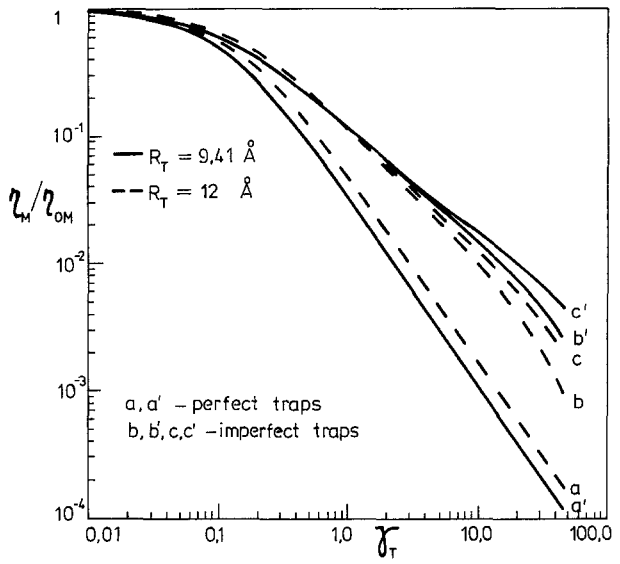

Fig. 5. Monomer fluorescence quantum yield versus trap concentration $\gamma_T = (\sqrt{\pi}/2)(C_T/C_0^{MT})$, calculated from Eqs. (5), (8'), and (9'). Curves b, b', c, and c'—energy migration (EM) and reversible energy transfer (RNET) taken into account. Curves c and c'—R_0^{TM} = 20 Å, R_0^{TT} = 25 Å, b, and b'—R_0^{TM} = 20 Å; R_0^{TT} = 0 Å. Curves a and a'—RNET neglected, $R_0^{TM} = R_0^{TT}$ = 0 Å.

plots of quantum yield η_M versus trap density γ_T for two values of the trap radius R_T. The curves are calculated from Eqs. (5), (8'), and (9') for the values of parameters listed in Table I and values of R_0^{TM} and R_0^{TT} given in the legend to Fig. 5. Let us note that for a fixed concentration γ_T, a greater monomer concentration γ_M corresponds to the system with lower R_T, and thus stronger energy migration and trapping processes are present (see curves a and a'). Altogether, the influence of the RNET process on the quantum yield η_M is stronger in this case (see curves a', b' and a, b). Thus, the effect of RNET on the monomer fluorescence quantum yield is considerable in a high concentration range, especially in systems with smaller values of R_T. In systems with greater values of the trap radius R_T, it may be necessary to include the NET process among trap molecules. This may be evident for greater values of critical radii R_0^{TM} and R_0^{TT}, especially in the high concentration region (cf. curves b, c and b', c' in Fig. 5). Needless to say, the systems consisting of traps of greater radii are not interesting. This is because in such a case it would be very difficult to explain the fluorescence quenching process correctly.

The results of emission anisotropy simulations showed a significant influence of reverse transfer on the courses of r_M/r_{0M}, especially for greater values of R_0^{TM} (see Fig. 3). Curves r_M/r_{0M}, calculated from Eq. (17) for $B' = 0$ and $B' > 0$, may be treated as upper and lower limits of possible r_M/r_{0M} values of the system in which reverse energy transfer takes place. The results of simulations reported here are the first step in investigations of RNET influence on emission anisotropy. It seems useful to elaborate the theory of the phenomenon as well as to carry out the experiment. The last task may be difficult with a view to strong overlap of the absorption and fluorescence bands of monomers and traps.

The fluorescence self-quenching process, known for years and widely discussed in the literature [1,7,44–48], is not yet satisfactorily elucidated. The most experimentally documented and theoretically explained is the phenomenon of fluorescence quenching by ground-state dimers [14,27,45,47–50]. However, in systems with weak fluorescence quenching, when absorption and emission bands do not change over a wide range of concentrations, the idea of statistical pairs as quenching centers is useful. It allows one to describe concentration changes in quantum yield with the trap radius R_T determined as a best-fit parameter [2–4,48].

FINAL REMARKS

Monte Carlo simulations of steady-state fluorescence quantum yield and emission anisotropy for systems containing monomers and statistical clusters (pairs and trimers) playing the role of imperfect traps for excitation energy were carried out. Numerical results were obtained for three-dimensional systems, assuming constant Förster distances R_0^{MM} and R_0^{MT} but different distances R_0^{TM} and R_0^{TT}. It was shown that the influence of reverse energy transfer may be significant in the range of high dye concentrations. A very good agreement between simulation results for quantum yield and the hopping model with correlations was found.

In the case of emission anisotropy, the agreement of the results of simulation with the prediction of the hopping model turned out to be only approximate. The calculated values of r_M/r_{0M} are low in comparison with the numerical data. This result is understandable, as expression (17) does not take into account the possibility of back-transfer of the excitation energy from traps to monomers M_i—the prime absorbers of the exciting light. It is useful to investigate both experimentally and theoretically the emission anisotropy in donor–acceptor systems in which direct and reverse energy transfer takes place. We hope to solve the problem of emission anisotropy in the framework of a systematic LAF theory of incoherent energy transport.

REFERENCES

1. C. Bojarski and K. Sienicki (1989) in J. F. Rabek (Ed.), *Photochemistry and Photophysics, Vol. 1*, CRC Press, Boca Raton, FL, pp. 1–57.
2. G. S. Beddard and G. Porter (1976) *Nature (London)* **260**, 366–367.
3. A. Penzkofer and Y. Lu (1986), *Chem. Phys.* **103**, 399–405.
4. J. Knoester and J. E. Van Himbergen (1987) *J. Chem. Phys.* **86**, 3571–3576; (1987) *J. Chem. Phys.* **86**, 4438–4441.
5. J. Knoester and J. E. Van Himbergen (1987) *J. Chem. Phys.* **86**, 3577–3582.
6. A. Penzkofer and W. Leupacher (1987) *J. Lumin.* **37**, 61–72.
7. D. R. Lutz, K. A. Nelson, C. R. Gochanour, and M. D. Fayer (1981) *Chem. Phys.* **58**, 325–334.
8. C. Bojarski (1984) *Z. Naturforsch.* **39a**, 948–951.
9. L. L. Shipman (1980) *Photochem. Photobiol.* **31**, 157–167.
10. C. S. French (1971) *Proc. Natl. Acad. Sci. USA* **68**, 2893–2897.
11. A. N. Rubinov, V. I. Tomin, and A. Buschuk (1982) *J. Lumin.* **26**, 377–391.
12. V. I. Yuzhakov (1979) *Russ. Chem. Rev.* (Engl. Transl.) **48**, 1076–1102.
13. L. V. Levshin and A. M. Saletskij (1990) *Opt. Spektrosk.* **68**, 354–358.
14. M. Kasha, H. R. Rawls, and M. A. El-Bayoumi (1965) *Pure Appl. Chem.* **11**, 371–392.
15. G. Zurkowska and C. Bojarski (1986) in *Proc. Int. Symp. Mol. Lumin. Photophys.*, Toruń, Poland, pp. 57–60.
16. C. Bojarski and G. Zurkowska (1987) *Z. Naturforsch.* **42a**, 1451–1455.
17. R. Twardowski and J. Kuśba (1988) *Z. Naturforsch.* **43a**, 627–632.
18. K. Sienicki and M. A. Winnik (1988) *Chem. Phys.* **121**, 163–174.
19. I. Ketskeméty, J. Dombi, R. Horvai, J. Hevesi, and L. Kozma (1961) *Acta Phys. Chem. Szeged* **7**, 17–24.
20. A. Budó and I. Ketskeméty (1957) *Acta Phys. Hung.* **7**, 207–223; (1962) *Acta Phys. Hung.* **14**, 167–176.
21. I. Ketskeméty and J. Kuśba (1977) *Acta Phys. Chem. Szeged* **23**, 375–382.
22. R. F. Loring, H. C. Andersen, and M. D. Fayer (1982) *J. Chem. Phys.* **76**, 2015–2027.
23. Th. Förster (1948) *Ann. Phys. (Leipzig)* **2**, 55–75.
24. C. Bojarski, A. Bujko, R. Bujko, and M. Cherek (1986) *Acta Phys. Hung.* **59**, 307–320.
25. J. R. Lakowicz (1986) *Principles of Fluorescence Spectroscopy*, Plenum Press, New York.
26. C. Bojarski and J. Dudkiewicz (1971) *Z. Naturforsch.* **26a**, 1028–1031; (1972) *Z. Naturforsch.* **27a**, 1751–1755.
27. C. Bojarski and G. Obermueller (1976) *Acta Phys. Polon.* **A50**, 389–411.
28. J. P. Webb, W. C. Mc Colgin, O. G. Peterson, D. L. Stockman, and J. H. Eberly (1970) *J. Chem. Phys.* **53**, 4227–4229.
29. C. Bojarski and J. Domsta (1970) *Z. Naturforsch.* **25a**, 1760; (1971) *Acta Phys. Hung.* **30**, 145–166.
30. R. Twardowski, J. Kuśba, and C. Bojarski (1982) *Chem. Phys.* **64**, 239–248.
31. D. L. Huber, D. Hamilton, and D. Barnett (1977) *Phys. Rev.* **B16**, 4642–4650.
32. D. L. Huber (1979) *Phys. Rev.* **B20**, 5333–5338.
33. R. Twardowski and C. Bojarski (1985) *J. Lumin.* **33**, 79–85.
34. A. I. Burshtein (1985) *J. Lumin.* **34**, 201–209.
35. M. D. Galanin (1950) *Trudy Fiz. Inst. Akad. Nauk USSR* **5**, 341–344.
36. A. Jabłoński (1970) *Acta Phys. Polon.* **A38**, 453–458.
37. E. L. Eriksen and A. Ore (1967) *Phys. Norvegica* **2**, 159–171.
38. C. Bojarski (1971) *Z. Phys. Chem. Neue Folge* **75**, 242–247.
39. C. Bojarski (1971) *Z. Naturforsch.* **26a**, 1856–1859.
40. C. Bojarski, J. Kuśba, and G. Obermueller (1971) *Z. Naturforsch.* **26a**, 255–259.
41. A. Kawski (1983) *Photochem. Photobiol.* **38**, 487–508.
42. C. Bojarski, J. Grabowska, L. Kułak, and J. Kuśba (1991) *J. Fluoresc.* **1**, 183–191.
43. A. Kawski, P. Bojarski, A. Kubicki, and C. Bojarski (1991) *J. Lumin.* **50**, 61–68.
44. Th. Förster (1951) *Fluoreszenz Organischer Verbindungen*, Vandenhoeck und Ruprecht, Göttingen (1951); (1966) *Proc. Int. Conf. Lumin., Akad. Kiado, Budapest*, Vol. 1, pp. 160–165.
45. V. L. Levshin (1963) *Izw. Akad. Nauk SSSR Ser. Fiz.* **27**, 540–550.
46. B. I. Makszantsev, E. A. Dynin, and V. M. Finkelberg (1981) *Chem. Phys.* **59**, 137–148.
47. M. D. Ediger and M. D. Fayer (1985) *Int. Rev. Phys. Chem.* **4**, 207–235.
48. K. Sienicki (1990) *Chem. Phys.* **146**, 79–87.
49. F. Lopez Arbeloa, P. Ruiz Ojeda, and I. Lopez Arbeloa (1989) *J. Lumin.* **44**, 105–112.
50. Th. Förster and E. König (1957) *Z. Elektrochem. Ber. Bunsenges. Phys. Chem.* **61**, 344–348.